

Real-time SPIDER: ultrashort pulse characterization at 20 Hz

Timothy M. Shuman, Matthew E. Anderson, Jake Bromage,
Chris Iaconis, Leon Waxer and Ian A. Walmsley

*Institute of Optics, University of Rochester, Rochester, NY 14627
USA*

shuman, slambo, bromage, iaconis, waxer, walmsley@optics.rochester.edu

Abstract: We present an implementation of spectral phase interferometry for direct electric-field reconstruction (SPIDER) which characterizes ultrashort optical pulses in the spectral or temporal domain at a rate of 20 Hz. This apparatus was used in real-time as a diagnostic tool to optimize our 1 kHz regeneratively amplified laser system for the shortest duration pulses.

© 1999 Optical Society of America

OCIS codes: (320.7100) Ultrafast measurements; (320.7110) Ultrafast nonlinear optics; (120.3180) Interferometry

References and links

1. T. Dunn, I. A. Walmsley and S. Mukamel, "Experimental determination of the quantum-mechanical state of a molecular vibrational mode using fluorescence tomography," *Phys. Rev. Lett.* **74**, 884-7 (1995); T. C. Weinacht, J. Ahn and P. H. Bucksbaum, "Measurement of the Amplitude and Phase of a Sculpted Rydberg Wave Packet," *Phys. Rev. Lett.* **80**, 5508-11 (1998).
2. A. Assion, T. Baumert, M. Bergt, T. Brixner, B. Kiefer, V. Seyfried, M. Strehle and G. Gerber, "Control of Chemical Reactions by Feedback-Optimized Phase-Shaped Femtosecond Laser Pulses," *Science* **282**, 919-22 (1998).
3. W. S. Warren, H. Rabitz and M. Dahleh, "Coherent Control of Quantum Dynamics: The Dream is Alive," *Science* **259**, 1581-9 (1993).
4. V. Wong and I. A. Walmsley, "Ultrashort-pulse characterization from dynamic spectrograms by iterative phase retrieval," *J. Opt. Soc. Am. B* **14**, 944-9 (1997).
5. J. L. A. Chilla and O. E. Martinez, "Direct determination of the amplitude and phase of femtosecond light pulses," *Opt. Lett.* **16**, 39-41 (1991).
6. D. N. Fittinghoff, J. L. Bowie, J. N. Sweetser, R. T. Jennings, M. A. Krumbugel, K. W. DeLong, R. Trebino and I. A. Walmsley, "Measurement of the intensity and phase of ultraweak, ultrashort laser pulses," *Opt. Lett.* **21**, 884-6 (1996).
7. R. Trebino, K. W. DeLong, D. N. Fittinghoff, J. N. Sweetser, M. A. Krumbugel and B. A. Richmand, "Measuring ultrashort laser pulses in the time-frequency domain using frequency-resolved optical gating," *Rev. Sci. Instr.* **68**, 3277-95 (1997).
8. M. A. Franco, H. R. Lange, J.-F. Ripoche, B. S. Prade, and A. Mysyrowicz, "Characterization of ultrashort pulses by cross-phase modulation," *Opt. Comm.* **140**, 331-40 (1997).
9. J. Rhee, T. S. Sosnowski, A. Tin and T.B. Norris, "Real-time dispersion analyzer of femtosecond laser pulses with use of a spectrally and temporally resolved upconversion technique," *J. Opt. Soc. Am. B* **13**, 1780-5 (1996).
10. C. Iaconis and I. A. Walmsley, "Spectral phase interferometry for direct electric-field reconstruction of ultrashort optical pulses," *Opt. Lett.* **23**, 792-5 (1998).
11. D. J. Kane, "Real-time measurement of ultrashort pulses using principal component generalized projections," *IEEE J. Selected Top. in Quant. Elec.* **4**, 278-85 (1999). A more rapid spectrogram acquisition and screen update has been reported at the Ultrafast Optics Conference, July 10-16, 1999, Ascona, Switzerland.
12. C. Iaconis and I. A. Walmsley, "Characterizing ultrashort optical pulses from the UV to the IR using SPIDER," talk presented at the OSA Annual Conference, Baltimore, MD (1998).
13. L. Gallmann, D. H. Sutter, G. Steinmeyer, U. Keller, C. Iaconis and I. A. Walmsley, "Pulses in the two-cycle regime from a SESAM-assisted KLM Ti:sapphire laser and sub-10-fs pulse characterization," in *Conference on Lasers and Electro-Optics*, OSA Technical Digest (Optical Society of America, Washington DC, 1999), pp.534-5.
14. C. Iaconis and I. A. Walmsley, "Self-referencing spectral interferometry for measuring ultrashort optical pulses," *IEEE J. Quantum Electron.* **35**, 501-9 (1999).

15. S. Kane and J. Squier, "Fourth-order dispersion limitations of aberration free chirped pulse amplification schemes," *J. Opt. Soc. Am. B* **14**, 1237-44 (1997).
 16. J. W. Goodman, *Introduction to Fourier Optics* (McGraw-Hill, New York, USA, 1988).
 17. M. Takeda, H. Ina and S. Kobayashi, "Fourier-transform method of fringe pattern analysis for computer based tomography and interferometry," *J. Opt. Soc. Am.* **72**, 1-12 (1982).
 18. C. Dorrer, S. Ranc, J. -P. Rousseau, C. Le Blanc and J. -P. Chambaret, "Single-shot real-time characterization using spectral phase interferometry for direct electric-field reconstruction," in *Conference on Lasers and Electro-Optics*, OSA Technical Digest (Optical Society of America, Washington DC, 1999), pp.533-4.
-

1 Introduction

Control of the amplitude and phase of ultrashort optical pulses is an important technology for many emerging areas of physics. For example, shaped ultrashort optical pulses are often used in both preparation [1] and measurement [2,3] in quantum control experiments. In this application, a knowledge of the electric field of the radiation is therefore critical. Because these and other experiments require control of optical pulse properties beyond simply the temporal duration and spectral bandwidth, and because this tailoring needs to be both accurate and stable from pulse to pulse, it is imperative that both the amplitude and phase profiles of the pulse be measured as far as possible in real-time. A technique capable of real-time characterization is therefore indispensable as a diagnostic tool for manual or automatic optimization or shaping of the laser pulses. In addition, a real-time characterization technique has a utility in everyday laboratory use. For instance, it could be used in a feedback loop for long term stabilization of the laser system output.

Many different techniques have been developed which are capable of characterizing ultrashort optical pulses [4-10]. The difficulty involved in implementing most of these techniques in real-time is the time required to collect and process the data. To date the fastest reported technique, frequency-resolved optical gating (FROG), achieved characterization rates of 2.3 Hz [11]. In general, interferometric methods require the collection of less data than spectrographic methods, and have direct inversion algorithms, so they have the potential to enable very rapid pulse shape reconstruction. In this paper, we realize this potential using spectral phase interferometry for direct electric field reconstruction (SPIDER). The SPIDER technique has been previously demonstrated on pulses from an 80 MHz oscillator [10], and on the fundamental and second-harmonic pulses from a 1 kHz regeneratively amplified laser system [12]. Recently, SPIDER has been used to characterize pulses in the two-cycle regime [13]. However, none of these demonstrations has investigated the capability of SPIDER for high speed, real-time pulse characterization.

This paper presents a new implementation of the SPIDER technique, called real-time SPIDER, which is capable of characterizing ultrashort pulses with an update rate of 20 Hz. A significant feature of this instrument is that it was built with common, inexpensive equipment which already exists in most laboratories. As a result, such performance can be achieved quickly, easily and cheaply.

The paper is structured as follows. Section 2 presents the SPIDER technique itself. Section 3 describes the real-time SPIDER apparatus and the particular elements which allow it to achieve real-time characterization. Section 4 presents the results from experiments performed with real-time SPIDER. In particular, several movies are included to demonstrate the utility of real-time SPIDER as a diagnostic tool in the laboratory. Lastly, Section 5 discusses the implications of this demonstration.

2 Theory

SPIDER [10] uses spectral shearing interferometry to retrieve the spectral phase of the incident pulse. This form of interferometry measures the interference between two pulses separated in time which are identical except for their central frequencies. This pulse pair is said to be spectrally sheared. The spectrum of this pulse pair is an interferogram signal of the form

$$S(\omega) = I(\omega + \Omega) + I(\omega) + 2\sqrt{I(\omega + \Omega)I(\omega)} \cos\{\phi(\omega + \Omega) - \phi(\omega) + \omega\tau\} \quad (1)$$

where Ω is the spectral shear (the difference between the central frequencies of the individual pulses in the pair), τ is the time delay between the pulses, $I(\omega)$ is the pulse spectrum and $\phi(\omega)$ is the spectral phase of the pulse. The time delay is introduced to facilitate phase recovery and is equivalent to the introduction of tilt fringes in spatial interferometry. A complete specification of the electric field of the pulse in the frequency domain is given by the pair of functions $\sqrt{I(\omega)}$ and $\phi(\omega)$. The former is easily measured (with the SPIDER apparatus or otherwise) and the latter can be extracted from the SPIDER interferogram. As will be shown, and is evident from the form of the interferogram given in Eq. (1), the spectral phase can be determined only at a series of frequencies separated by the shear, Ω . That is, inversion of the SPIDER data yields a sampling of the spectral phase at points $\{\phi(\omega_i), \phi(\omega_i + \Omega), \phi(\omega_i + 2\Omega), \dots\}$. However, this is a sufficient set to uniquely specify the pulse provided it has compact support in time, a *sine qua non* for ultrashort pulse characterization [14].

The key to the SPIDER technique is generating the spectrally sheared pulse pair in the laboratory. In order to produce a shear of the required magnitude (typically a significant portion of the pulse spectral width, or for femtosecond pulses several THz), a nonlinear process must be used. Both upconversion and downconversion have been used for this purpose, depending on the central wavelength of the pulses being characterized. By mixing two properly conditioned beams in a nonlinear crystal, the resulting sum or difference frequency radiation consists of a spectrally sheared pulse pair. One of the beams incident on the crystal is a pair of identical pulses (replicas of the pulse being characterized), separated completely by time delay τ . The other beam contains a highly chirped pulse. The chirp on this pulse should be large enough to satisfy two conditions. First, the duration of the chirped pulse should be much longer than the time delay τ . Second, during each of the replica pulses, the chirped pulse is essentially monochromatic. This ensures that when these two beams mix in the crystal, each pulse in the pair mixes with a different frequency in the chirped pulse. The pulses emerging from the crystal, therefore, are each shifted to a different frequency, i.e. they are spectrally sheared. The spectrum of the pair has exactly the form given in Eq. (1). Figure 1 contains a plot of a simulated interferogram of this functional form.

The magnitude of the spectral shear generated in this manner is a function of two parameters: the separation between the pulses in the pair and the amount of chirp on the stretched pulse. For pulses stretched using a typical grating stretcher in which second order dispersion dominates, the exact value of the shear is equal to

$$\Omega = -\frac{\tau}{2\phi_2} \quad (2)$$

where τ is the separation between the pulses and ϕ_2 is the second-order dispersion present on the chirped beam. In this case, the value of ϕ_2 is determined from the relations stated in [15].

Once the interferogram signal is resolved, it is sampled with a detector at the output of the spectrometer or monochromator. There are two issues involved in sampling the

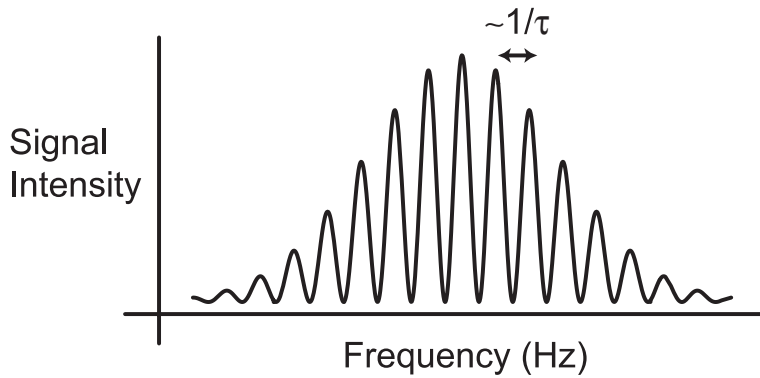


Fig. 1. Plot of an ideal interferogram of the form shown in Eq. (1). The nominal spacing between the fringes is $1/\tau$. Any deviations from this spacing are due to a nonconstant spectral phase profile on the pulse being characterized.

interferogram so the spectral phase is recoverable from the sampled data. First, the data must be sampled above the Nyquist limit (> 2 points per fringe). This condition is satisfied by properly selecting the pulse pair separation τ , taking into account the spectrometer resolution. In addition, the requirements of the Whittaker-Shannon sampling theorem must be satisfied [16] by generating a proper spectral shear. This guarantees the uniqueness of the reconstructed field. If the shear is too large, the sampling theorem is violated and the spectral phase cannot be recovered exactly. On the other hand, if the shear is too small, the interferogram will not be sampled densely enough to resolve the deviations from the nominal spacing, making the spectral phase recovery more susceptible to errors in the presence of noise. The value of the shear is adjusted by changing the second-order dispersion on the chirped pulse. When using a stretcher to generate this pulse, this can be done simply by adjusting the separation between the gratings, which affects the shear value according to Eq. (2).

After the interferogram is sampled properly, the spectral phase information needs to be extracted from this data. A direct procedure for doing this was developed in [17]. The first step in this procedure is to Fourier transform the sampled data. Three peaks, separated in time, result: a single "DC" peak due to the constant term in Eq. (1) that occurs near zero time ($t = 0$) and two "AC" sidebands due to the cosine term that occur at $t = \pm\tau$. Only the sideband peaks contain the phase information and each of them contains all of the information. Therefore, a supergaussian filter is applied to remove the DC peak and one of the AC sidebands. The remaining sideband is inverse Fourier transformed back to frequency. The phase profile of this frequency data is exactly the argument of the cosine term in Eq. (1). The phase term linear in the pulse separation (the $\omega\tau$ term) can be removed by subtracting a calibration trace. The remaining phase data is the phase difference between 2 frequencies in the pulse pair separated by the spectral shear. Through a concatenation of this phase difference data, the spectral phase can be recovered [14]. If the temporal profiles are desired, a spectrum of the unknown pulse must be measured. The spectral phase and spectrum can be combined to form the complete spectral field. Simply Fourier transforming this function yields the temporal field, from which the temporal intensity and phase can be extracted.

The SPIDER algorithm also succeeds in reconstructing complicated or noisy pulse shapes, provided the requirements imposed by the Whittaker-Shannon sampling theorem are met. For example, SPIDER has recently been used to reconstruct ultrashort pulses with Π phase jumps in a single-shot configuration [18]. Simulations show that SPIDER is robust with respect to additive noise as well as multiplicative noise, provided

the sampling constraints are satisfied. For example, in the case of additive noise an SNR of 6 for the interferogram yields an rms spectral phase error of $\Pi/30$, and in the case of multiplicative noise an SNR of 4 leads to an rms phase error of $\Pi/20$ on transform limited pulses.

3 Experiment

The laser system used for the real-time SPIDER experiment was a 1 kHz Ti:sapphire regeneratively amplified laser system emitting pulses 50-60 fs in duration and centered at a wavelength of 830 nm. Figure 2 shows a schematic of the real-time SPIDER apparatus. This apparatus is similar to those used in previous implementations of SPIDER. The first optical element in the apparatus is a thin glass etalon, splitting the incident beam into 2 pieces. The reflected beam is the pair of identical pulses. These pulses are sent through an adjustable delay line and $\lambda/2$ waveplate to rotate their polarization. The beam transmitted through the etalon becomes the chirped pulse, after passing through a double-pass grating pair stretcher (two 1200 groove/mm gratings separation by 4.5 cm, which stretch the pulse from about 100 fs to 12.7 ps). Since these beams have orthogonal polarizations, they are recombined using a thin film polarizer and are focused into a 250 μm thick type II BBO crystal. The upconverted sheared pair is recollimated and sent into a 1/4 m, 0.5 \AA resolution spectrometer (Instruments SA HR320 with a 1800 groove/mm grating). The spectral interferogram is sampled with a linear detector array. The sampled data is then fed into a National Instruments DAQ card (PC-LPM-16) with a maximum sampling rate of 50,000 samples per second. The data acquired by the computer is processed by several LabVIEW programs (called virtual instruments or VIs) which display the reconstructed pulses on the computer screen.

There are two significant differences between the real-time apparatus and the apparatus used in previous demonstrations of SPIDER. First, an etalon is used to generate the identical pulse pair instead of a Michelson interferometer with mismatched arms. There were two reasons for making this change. First, an etalon requires no alignment. Second, the etalon is more stable mechanically than a Michelson. A fluctuating time delay between the two pulses in the sheared pair adds noise to the recovered spectral phase profile. The separation of the replicas is equal to

$$\tau = \frac{2nL}{c} \quad (3)$$

where n is the refractive index of the etalon, L is its thickness and c is the speed of light. The only deviations in the pulse separation from this value are due to variations in the etalon thickness across the beam spot. It is easy to test for this, however. Simply focusing the entire reflected beam from the etalon into a spectrometer and recording the spectrum will yield an interferogram with fringes spaced at $2\pi/\tau$ (in angular frequency). The visibility of these fringes will be high unless the etalon thickness is nonuniform. The etalon used in real-time SPIDER was a 200 μm thick fused silica etalon (CVI part no. ET-25.4-0.2-UV) which generated a measured pulse separation of 1.8 ps. If the etalon introduces additional dispersion onto the pulses, half of this dispersion is compensated for in the calibration of the device. However, due to the thinness and material of the etalon used here, its dispersion can be neglected.

The second modification is the use of a linear detector array to sample the interferogram, instead of a scanning monochromator. There are two main issues involved in selecting a suitable detector array. The first is the sensitivity of the array at the upconverted wavelength. Second, the pixel width must be sufficient to allow the entire interferogram to be sampled at the focal plane of the spectrometer. Note, although the values of τ and Ω are selected to satisfy the sampling limits, the choice of these values

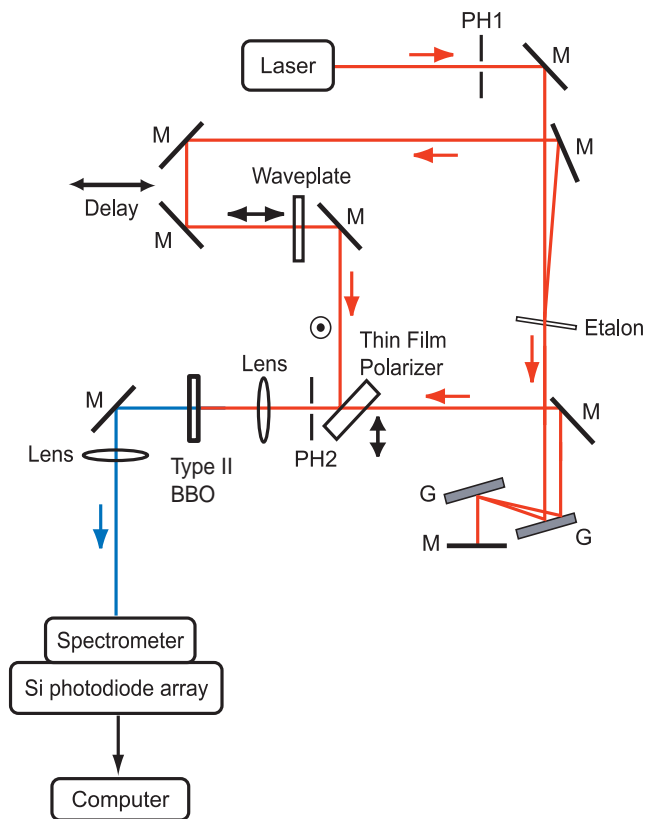


Fig. 2. Schematic of the real-time SPIDER apparatus. Notation: M=mirror, G=grating, PH=pinhole.

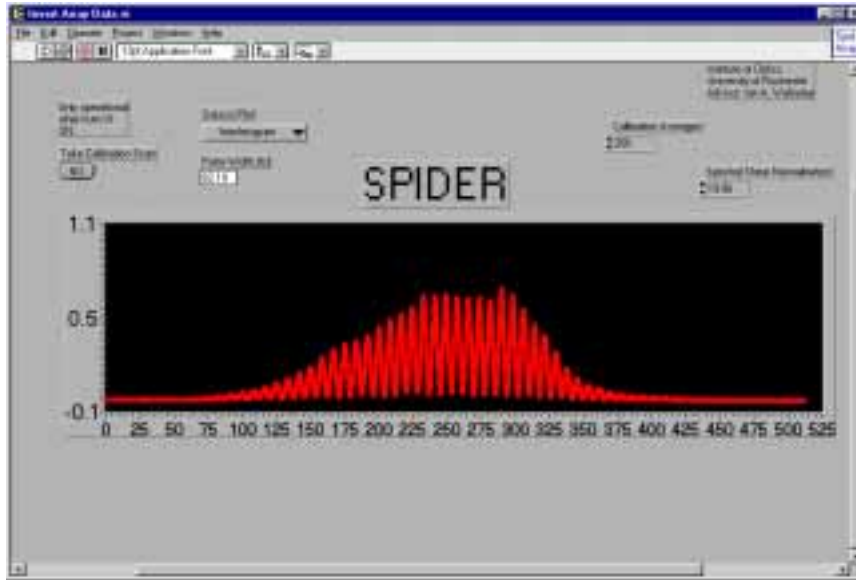


Fig. 3. Computer screen displaying the SPIDER LabVIEW Control program, showing the sampled interferogram. The vertical axis is the pixel voltage from the detector and the horizontal axis is the pixel number. The pixel range 150-350 corresponds to an upconverted wavelength range of 410-420 nm.

is also a function of the pixel width of the detector array. A 512 pixel, silicon photodiode array with $25 \mu\text{m}$ wide pixels was used in our experiments (Hamamatsu model S3903-512Q).

The sampled interferogram data is sent into the computer and processed by a set of LabVIEW VIs which return the reconstructed pulse profiles. Figure 2 shows a screen shot from the LabVIEW control VI where the sampled interferogram from the detector array is plotted (as the array voltage versus pixel number). Due to SPIDER's direct inversion algorithm, using LabVIEW to reconstruct the spectral phase is relatively simple. The LabVIEW VI which does this uses the built-in FFT routine and other functions which eliminate the need to import any custom C code.

4 Results

The ability of this SPIDER apparatus to perform complete ultrashort pulse characterization at 20 Hz can only be fully appreciated by seeing the instrument working. To this end, three movies are included which demonstrate the utility of real-time SPIDER as a diagnostic tool in the laboratory. Each of these movies is a direct recording of the computer display output. Figure 4 contains a screen shot from the first movie. Here, the spectral phase of the laser pulse is displayed as the chirp is adjusted by changing the grating separation in the compressor stage of the laser system. As can be seen in the movie, there is an optimum grating separation where the spectral phase is flattest and the pulses shortest. This single demonstration shows that real-time SPIDER may be used as a diagnostic and optimization tool for repetitive pulsed laser systems.

Although flattening the spectral phase is the most accurate way to optimize the laser system, the pulse intensity is often a more intuitive way to monitor the laser system. Figure 5 contains a screen shot from a movie where instead of the spectral phase the temporal intensity is displayed as the grating separation is adjusted. Again, there is a clear optimum position where the pulse is at its shortest, and this, of course, is the same

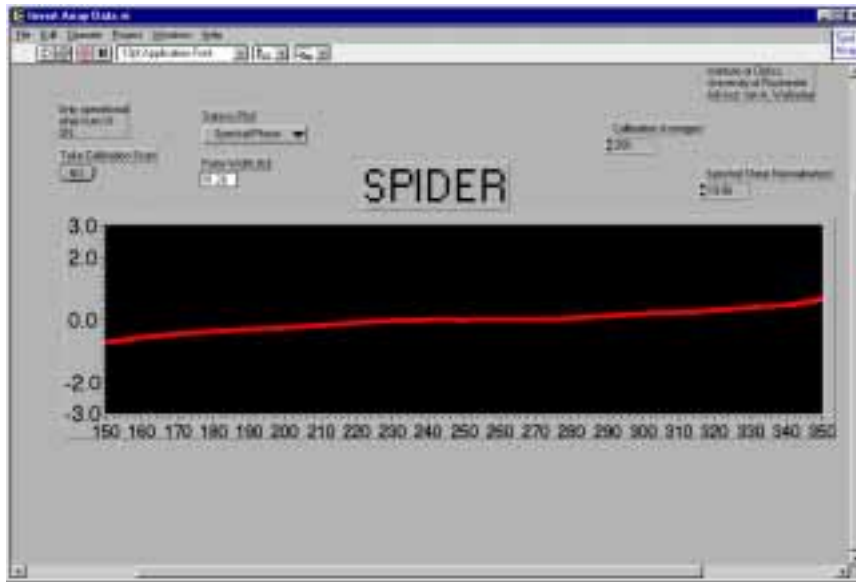


Fig. 4. Movie of the pulse spectral phase as the dispersion on the pulse is changed by adjusting the grating separation in the compressor (2.5 MB QuickTime movie).

position that flattens the spectral phase.

Figure 6 contains a screen shot from the third movie. This movie shows the temporal intensity profile of the pulse as a 1.5 inch thick piece of glass is inserted into and removed from the laser beam. Note the increase in the pulse duration due to the added dispersion and the reduction in the intensity due to the reflections at the air-glass interfaces.

Both the characterization rate and the accuracy of the pulse reconstructions were verified experimentally. To verify the characterization rate of the apparatus, a chopper wheel was inserted into the beam. Adding the chopper wheel causes the data plotted on the computer screen to beat in time. The frequency of this beating is equal to the difference between the chopping frequency and the update rate of the apparatus. Verifying the 20 Hz update rate involved ramping the chopper frequency while observing the beat frequency. At 10 Hz, a beat frequency of 10 Hz was observed, while at 20 Hz, a beat frequency approaching zero was observed. These results prove the real-time SPIDER system, including data collection, inversion and computer screen update can operate at 20 Hz.

In order to determine the accuracy of the pulse reconstructions returned by real-time SPIDER, a known amount of dispersion was added to the laser pulses. The spectral phase returned by SPIDER was then compared to the expected spectral phase due to the added dispersion. One such comparison is plotted in Figure 7. Here the retrieved spectral phase (in red) is plotted against the expected spectral phase (in blue) due to a 1270 μm change in the grating separation in the laser system's compressor. The black bars denote the bandwidth (FWHM) of the pulse spectrum. The RMS phase error across the plot (which covers the $1/e^2$ extent of the spectrum) is equal to 0.128 radians. This phase error corresponds to an error in the reconstruction pulsewidth of 6%. However, since the meaning of the phase diminishes as the pulse intensity decreases, a better measure of the error is across the spectral bandwidth. Across this region, the RMS phase error is equal to 0.062 radians, which corresponds to less than 2% error in the reconstructed pulsewidth.

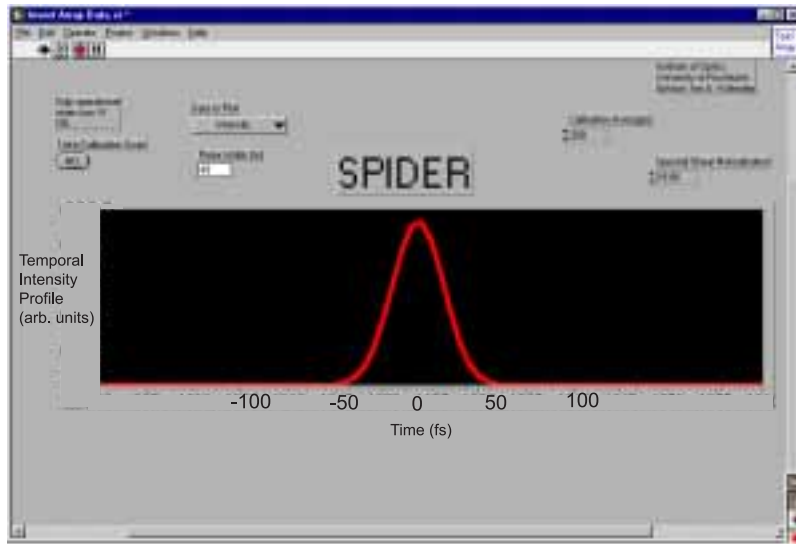


Fig. 5. Movie of the temporal intensity of the pulse as the dispersion on the pulse is changed by adjusting the grating separation in the compressor (1.6 MB QuickTime movie).

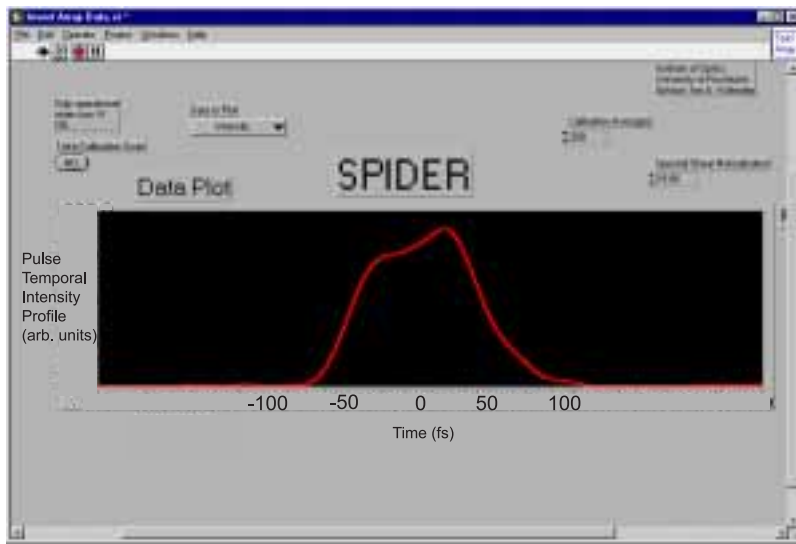


Fig. 6. Movie of the temporal intensity with and without a 1.5 inch thick piece of glass in the laser beam. (663 kB QuickTime movie).

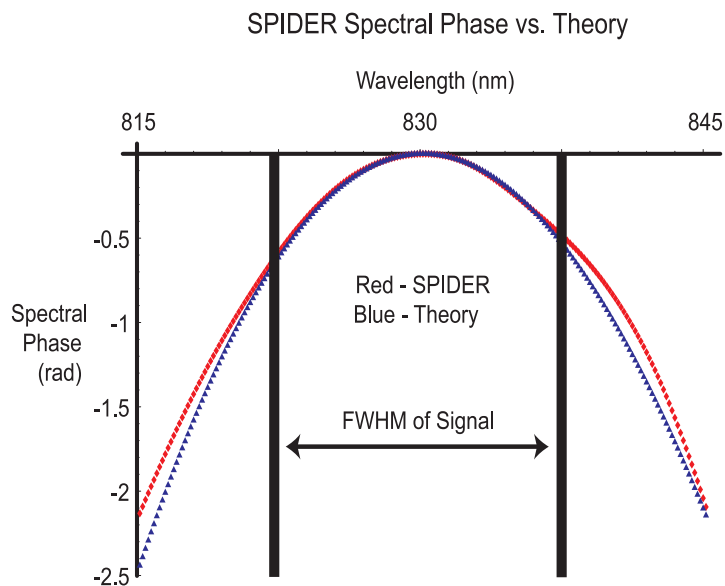


Fig. 7. Comparison of the spectral phase retrieved from real-time SPIDER and the expected spectral phase for a $1270 \mu\text{m}$ change in the grating separation in the compressor. The RMS phase error in the reconstruction across the $1/e^2$ extent of the spectrum is 0.128 radians which corresponds to a 6% error in the reconstructed pulsewidth.

5 Conclusions

This paper has presented an implementation of the SPIDER technique capable of real-time characterization of ultrashort pulses at a rate of 20 Hz. There are several ramifications of pulse characterization at this speed. First, optimization or adjustment of the laser system is much easier and faster using the output of real-time SPIDER as a diagnostic tool. Second, since the apparatus was built with common, inexpensive equipment, this apparatus can be built quickly, easily and cheaply. Third, the high characterization rate of this apparatus will allow real-time computer controlled feedback of laser systems for optimization and pulse shaping. Lastly, the 20 Hz rate achieved here is not a fundamental limit of the SPIDER technique. We expect that by utilizing a commercial DSP board to perform the data acquisition and processing tasks, the characterization rate of this apparatus could be improved to upwards of several hundred characterizations per second.

6 Acknowledgments

The authors would like to thank Luis de Araujo for assistance in preparing this manuscript. This work was supported by a grant from the National Science Foundation under the GOALI program.